Journal of Geophysical Research: Biogeosciences

RESEARCH ARTICLE
10.1029/2018JG004403

Key Points:
- Variation in isoprenoid and acetogenic lipid hydrogen isotope values exceeds leaf water hydrogen isotope variability
- Dominant osmoregulatory strategies show a strong correlation with the hydrogen isotope compositions of leaf wax biomarkers
- Leaf wax biomarkers are valuable tools for investigating metabolic adaptations to environmental stress in modern and ancient environments

Supporting Information:
- Supporting Information S1

Correspondence to:
Y. Eley,
y.eley@bham.ac.uk

Citation:
Eley, Y., White, J., Dawson, L., Hren, M., & Pedentchouk, N. (2018). Variation in hydrogen isotope composition among salt marsh plant organic compounds highlights biochemical mechanisms controlling biosynthetic fractionation. *Journal of Geophysical Research: Biogeosciences*, *123*. https://doi.org/10.1029/2018JG004403

Received 16 JAN 2018
Accepted 14 JUL 2018
Accepted article online 1 AUG 2018

Variation in Hydrogen Isotope Composition Among Salt Marsh Plant Organic Compounds Highlights Biochemical Mechanisms Controlling Biosynthetic Fractionation

Yvette Eley[1,2,3], Joseph White[4], Lorna Dawson[5], Michael Hren[3], and Nikolai Pedentchouk[2,6]

[1]School of Geography, Earth and Environmental Sciences, University of Birmingham, Birmingham, UK, [2]School of Environmental Sciences, University of East Anglia, Norwich, UK, [3]Center for Integrative Geosciences, University of Connecticut, Storrs, CT, USA, [4]Department of Biology, Baylor University, Waco, TX, USA, [5]James Hutton Institute, Aberdeen, UK, [6]Institute of Plant Physiology, Russian Academy of Sciences, Moscow, Russia

Abstract Hydrogen isotopes of plant-derived biomarkers can vary by >100‰ at a single location. Isotope fractionation associated with the movement of water in plant leaves cannot account for this variability alone. Biochemical processes therefore must play a fundamental role in controlling hydrogen isotope fractionation during secondary compound biosynthesis. Different biosynthetic pathways utilize discrete hydrogen pools and occur within distinct cell compartments. We analyzed hydrogen isotope compositions of C_{16} and C_{18} fatty acids and phytol from seven salt marsh plants and compared these data with (i) leaf water and *n*-alkane δ^2H, (ii) leaf carbon and nitrogen contents, and (iii) nitrogen isotopes of bulk tissue, to evaluate the relationship between biochemical processes, cellular compartmentalization, and hydrogen isotope fractionation. Interspecies variation in chloroplastic fatty acids and phytol δ^2H exceeds leaf water δ^2H, indicating that different commitments of metabolites among species at branching points in chloroplast metabolic processes may be important determinants of lipid δ^2H values. Dominant osmoregulatory strategies, in particular, show strong correlation with leaf wax *n*-alkane δ^2H. Species that preferentially produce nitrogenous compounds (dicots/shrubs) as protective solutes have ^2H-enriched *n*-alkanes relative to species that produce mainly carbohydrates (monocots). *n*-Alkane δ^2H values, in combination with $\delta^{15}N$ data and elemental (C, N) composition, together provide information about biochemical environmental adaptations exhibited by different higher plant species in response to environmental stresses. Thus, while spatial and temporal integration of biomarkers may produce an isotopic record of ecosystem function, biomarkers from individual plant or microbial remains may hold additional details into biologic function and adaptation to ancient environments.

1. Introduction

The hydrogen isotope composition of *n*-alkyl lipids from terrestrial plants are widely interpreted to reflect source water δ^2H values, with modification by a range of processes within the plant such as root uptake, transpiration, and leaf water evaporative enrichment (Kahmen et al., 2013; McInerney et al., 2011; Sachse et al., 2010, 2012). The δ^2H value of sedimentary leaf wax biomarkers has been used to reconstruct the hydrogen isotope composition of paleoprecipitation (e.g., Feakins et al., 2014; Pagani et al., 2006; Schefuss et al., 2011), the availability of moisture (Niedermeyer et al., 2016; Tierney et al., 2011; Tierney & deMenocal, 2013), and paleoelevation (Hren et al., 2010; Kar et al., 2016). Recent studies of extant plants growing at a single geographical location have revealed that variation in δ^2H_{wax} can exceed 100‰, which cannot be fully accounted for by processes controlling the isotopic composition of soil, xylem, or leaf water (Eley et al., 2014; Oakes & Hren, 2016). These studies highlight the significant influence that biochemical mechanisms may exert over the δ^2H of leaf wax biomarkers. Indeed, studies of other photosynthetic organisms regularly invoke differences in cellular metabolic strategies in response to observed variation in lipid δ^2H values (Fischer et al., 2013; Zhang et al., 2009; Zhang & Sachs, 2007).

Leaf wax biomarker-based paleoenvironmental reconstructions are based on an "ecosystem average" that incorporates plant material both spatially (e.g., in terms of catchment area) and temporally over hundreds to thousands of years of soil formation. As a result, specific differences in individual plant biochemistry are

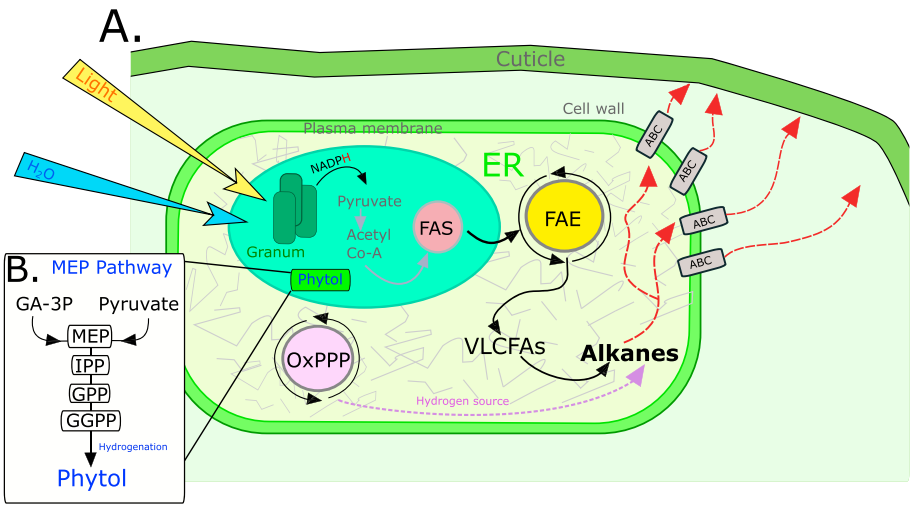

Figure 1. (a) Simplified schematic showing the compartmentalization of lipid production for the biomolecules analyzed in this study. FAS = fatty acid synthase; FAE = fatty acid elongase; ER = endoplasmic reticulum; VLCFAs = very long chain fatty acids; OxPPP = oxidative pentose phosphate pathway; ABC = ABC transporters thought to move alkanes to the cell wall (Kunst & Samuals, 2009). (b) Insert showing the conceptualized biosynthesis of phytol in the chloroplast. GA-3-P = D-glyceraldehyde-3-phosphate; MEP = 2-C-methyl-D-erythritol-4-phosphate; IPP = isopentenyl pyrophosphate; GPP = geranyl phosphate; GGPP = geranylgeranyl phosphate.

likely to be lost in the averaging process. While empirical observations of soil *n*-alkanes show a systematic variation with the hydrogen isotope composition of environmental water (e.g., Douglas et al., 2012; Garcin et al., 2012), the fact remains that at the individual plant level, other factors exert strong influences over *n*-alkane hydrogen isotopes (Eley et al., 2014). A more detailed appreciation of the biological mechanisms that control leaf wax lipid hydrogen isotope values (and the way these perturbations are recorded in the *n*-alkane hydrogen isotope signal) has the potential to expand the organic molecular toolkit for paleoenvironmental investigations, enabling reconstruction of factors such as plant energy budgets and metabolism (Cormier et al., 2018)

Water is the prima facie source of hydrogen in all organic compounds synthesized by plants (Schmidt et al., 2003), and hydrogen ions from photosynthetic water fission are the primary source of hydrogen incorporated into plant NADPH (Luo et al., 1991; Schmidt et al., 2003; Figure 1). However, photolysis is not the sole source of hydrogen available for $NADP^+$ reduction in plants. $NADP^+$ can be reduced to NADPH by the oxidation of sugars in the pentose-phosphate cycle (OPPP), where the hydrogen derives from C-bound H contained within sugars (Schmidt et al., 2003; Sessions, 2006; Sessions et al., 1999). These diverse hydrogen sources give rise to differences in the isotopic composition of NADPH among plant compartments (Schmidt et al., 2003) and have been proposed as mechanisms to account for interspecies variation in leaf wax *n*-alkane δ^2H values (Newberry et al., 2015).

The biochemical adaptations used by plants to ameliorate environmental stresses results in the production of distinct carbon pools across cell compartments, containing organic compounds with widely varied hydrogen isotope compositions. As a result, these responses are likely to play an important role in controlling leaf wax biomarker hydrogen isotope systematics. However, recent studies have often focused on one type of plant when considering the potential significance of this biological response on biomarker hydrogen isotope values, for example, mangroves (Ladd & Sachs, 2012, 2015). The production of a suite of osmolytes (e.g., proline mannitol, sorbitol, glycine betaine, and pinitol) in response to stresses including salinity, drought, high UV light, and heavy metal toxicity is critical to plant survival (Ashraf & Foolad, 2007; Parida & Das, 2005). These protective solutes are an important draw on the reducing power of the cells of many plants facing a wide range of environmental stresses (Parida & Das, 2005). Studies of stable isotope fractionation in biological systems have shown that the composition of specific compounds can be strongly influenced by the flux of material through branch points in reaction networks (Hayes, 2001; Hobbie & Werne, 2004; Wing & Halevy, 2014). Interspecies differences in the proportions of protective solutes produced, and seasonal shifts in their

demand, have the potential to drive changes in the hydrogen isotope composition of *n*-alkanes through changes in the fluxes of precursor compounds such as pyruvate through branch points of biosynthetic reaction networks (Diefendorf et al., 2011; Good & Zaplachinski, 1994; Rhodes et al., 1986). Equally, previous studies have concluded that differences in hydrogen isotope fractionation between source water and *n*-alkanes could be driven by biochemical differences at the genetic level, with distinct lineages (e.g., monocots and lycopods) differing in terms of their allocation of photosynthate to metabolic and biochemical functions (Gao et al., 2014).

In the plant acetogenic lipid pathway, acetyl-CoA is the precursor for fatty acids (Harwood, 1988; von Wettstein-Knowles et al., 2006), which in turn are the precursors for all other acetogenic lipids (Quemerais et al., 1995; Schmidt et al., 2003; Zhang et al., 2009). Investigation of compounds metabolized upstream in the biochemical reaction network generating acetogenic lipids (e.g., short chain fatty acids; Figure 1) permits evaluation of the stage in the biosynthetic process at which interspecies variation in δ^2H value is established. Here we compare the hydrogen isotope composition of acetogenic lipids with that of compounds produced by other reaction networks, such as the 1-deoxy-d-xylose-5-phosphate (DOXP) pathway generating phytol (Chikaraishi et al., 2005, 2009). Critically, phytol is produced during chlorophyll biosynthesis in the chloroplast (Chikaraishi et al., 2005, 2009), using a different suite of precursors from the acetogenic pathway. We use these data to inform our hypotheses regarding potential biochemical mechanisms operating in the chloroplast and/or the cytosol that may drive interspecies differences in biomolecule hydrogen isotope values. Finally, it has been previously established that the salt marsh species studied here produce different dominant protective solutes (e.g., carbohydrates versus nitrogenous compounds) in response to environmental stress (Briens & Larher, 1982). We investigate whether leaf wax hydrogen isotopes show any systematic variation with the nature of dominant protective solutes, providing a first-order evaluation of whether these biochemical adaptations are important for interpreting lipid biomarker profiles in both modern and ancient plants.

Here we quantify variability in the hydrogen isotope composition of phytol, C_{16} and C_{18} fatty acids, and bulk plant tissue from seven C_3 and C_4 plants growing in a temperate UK salt marsh. Phytol was selected as it is produced via the isoprenoid pathway in the chloroplast as a phytyl side-chain of chlorophylls, using a distinct pool of NADPH as a source of hydrogen (Chikaraishi et al., 2009). C_{16} and C_{18} fatty acids, produced in the chloroplast and transported to the cytosol, were of interest as they represent compounds utilized early in the biosynthetic pathway producing *n*-alkanes (Shepherd & Griffiths, 2006). We compare these data with leaf water, xylem water, and *n*-alkane δ^2H values previously reported in Eley et al. (2014), to evaluate whether the patterns of ^{2}H-enrichment and depletion are coherent across all compound classes produced in different cell compartments. Finally, we investigate the preferred osmolytes produced by each species, alongside empirical observations of their percentage carbon and nitrogen content and bulk nitrogen isotope composition, to consider whether differences in biochemical responses to environmental stress can influence leaf wax hydrogen isotope values. Plant C:N ratios, and differences in overall C and N content, can reflect variation in the proportion of structural carbohydrates (e.g., Dungait et al., 2008), while differences in nitrogen isotope compositions can be indicative of variation in the source of nitrogen utilized, the method of uptake, and, potentially (as we use it here), the relative proportion of nitrogenous compounds produced by a plant in response to external stress given that nitrogenous compounds are typically enriched in ^{15}N relative to other biological compounds in phototrophic cells (Macko et al., 1986, 1987).

2. Materials and Methods

2.1. Site Description and Sampling Strategy

The sampling site used for this study is Stiffkey salt marsh on the north Norfolk coast of the UK, an open coast back-barrier marsh described in detail in Eley et al. (2014). We sampled seven plant species from the salt marsh site throughout the duration of the study. These species were selected as they were representative (in terms of ground cover) of each of the sub-habitats (low marsh, mid marsh and upper marsh) targeted during sampling. Further, these species have distinct leaf morphologies (e.g., succulents and broad leaved grasses), life strategies (e.g., evergreen, perennial, and annual), and carbon metabolisms (C_3 versus C_4).

Working with the tidal regimes, sampling was carried out at a similar time of day throughout the entire study, and care was taken to select healthy leaves, with no obvious evidence of damage or disease. Fresh leaf

material for phytol analysis was collected in August 2012. After collection, plant samples for phytol extraction were placed into sample bags and immediately stored in dry ice in the field to prevent enzymatic activity. Upon returning samples to the laboratory, they were transferred directly to a low temperature freezer maintained at −80 °C, until required for analysis.

2.2. Extraction of Phytol and Fatty Acids

Phytol extraction was carried out using previously established methods (Chikaraishi et al., 2004, 2009). Briefly, fresh frozen plant leaves were ground into a powder using the cryogenic mill and extracted with acetone for 2 min. Ultrapure water was added, and the extracted pigments were reextracted from the acetone/water mix using hexane. To ensure complete extraction of the pigments, the powdered plant material was then placed in acetone and stored for 24 hr in a freezer until colorless. The hexane solutions were filtered with a Whatman GF/F filter (0.7 μM pore size) and evaporated under N_2. Samples were redissolved in methanol, and chlorophylls were precipitated by the sequential addition of 1,4dioxane/H_2O (1:1, *v*/v) and removed via filtration as before. The remaining solutions were extracted with hexane from the MeOH/H_2O mix, to remove the lipids and carotenoids. Solutions were saponified with 0.5 M KOH in MeOH/H_2O (95/5, *w*/w) at 75 °C for 4.5 hr. After adding H_2O to the saponified solutions, phytol was extracted using hexane/DCM (2:1, *v*/v) and acetylated at 75 °C for 8 hr. Phytol samples were analyzed on a Perkin Elmer Clarus 500 GC/MS, equipped with a DB-5 capillary column (30 m x 0.32 mm i.d. x 0.25 μm film), using helium as a carrier gas. Retention times compared to those obtained for a phytol standard (>97% purity, Sigma Aldrich). During analysis, the GC oven temperature was programmed from 50 °C, and then increased at a rate of 30 °C/min until it reached 120 °C. A second ramp then took the temperature to 310 °C at a rate of 6 °C/min, with this final temperature held for 15 min.

Fatty acid samples were extracted and methylated in a single step (Garcés & Mancha, 1993). Dried, chopped plant material was placed in a sample vial, and 3.3 mL of MeOH:toluene:DMP:H_2SO_4 (39:20:5:2 *v*/v) was added. The vials were then made up to 5 mL with heptane. Vials were flushed with N_2 gas, sealed, and then placed in a water bath at 80 °C for 2 hr. After agitation, the surface heptane layer containing the fatty acid methyl esters (FAMEs) was removed and concentrated to ~200 μ under N_2. Sample peaks were identified by comparison to retention times of a Supelco grain FAME standard (Sigma Aldrich) using a Carlo Erba GC/MS complete with a SGE BPX70 column (0.22 mm I.D., 0.25 μm film thickness, 30 mm length). The GC detector was held at 300 °C during analysis, while the injector was maintained at 210 °C. The oven had an initial temperature of 50 °C, which was held for 2 min. The oven temperature was then raised to a 240 °C at a rate of 7 °C per min, and then held isothermal for 18 min.

2.3. Hydrogen Isotope Analysis of Phytol and Fatty Acids

All isotope values reported in this study are expressed in delta notation, as shown in equation (1):

$$\delta^{A}X_{STD} = \frac{R_{Sample}}{R_{Standard}} - 1 \quad (1)$$

where δ represents the abundance of isotope *A* of element *X* in a given sample relative to the abundance of isotope *A* in an accepted reference standard (Hayes, 2001).

The δ^2H of derivatized phytol and FA samples was analyzed using a ThermoFisher Delta V Advantage isotope-ratio mass spectrometer interfaced with GC-Isolink Trace GC Combustion and High temperature conversion (HTC) system operating at 1400 °C. All GC oven temperature programs used for isotope measurements were identical to GC/MS methods described above, with helium again used as a carrier gas. For phytol, the DB-5 column (described above) was used for analysis, while for fatty acids we used a DB-23 column (also made by Agilent Technologies). δ^2H values are based on a minimum of duplicate measurements of well-resolved peaks and reported on the V-SMOW scale, based on a standard mixture of an *n*-C_{16} to *n*-C_{30} alkanes with known hydrogen isotope values (Arndt Schimmelmann, Indiana University, USA). Root-mean-square error for $^2H/^1H$ measurements of this standard was 4.0‰ (n = 780). Due to low concentrations of phytol in the salt marsh extracts, sample duplicates were combined after GC/MS analysis to ensure sufficient peak intensity for hydrogen isotope analysis. Standard error of analytical replicates of phytol samples did not exceed 4‰ (Table S1). Analytical reproducibility of triplicate measurements of well-resolved fatty acid peaks from the same sample did not exceed 6‰, while sample replicates from the same plant species typically did

not differ by more than 6‰. To correct for the addition of hydrogen during derivatization of these compounds, phthalic acid of known isotopic composition (Schimmelmann, Indiana, USA) was also derivatized using the same reagents. The isotope fractionation between leaf water and phytol, defined as $\varepsilon_{lw/phytol}$, was calculated as shown in equation (2):

$$\varepsilon \mathrm{lw/phytol} = \frac{\left({}^2H/{}^1H\right)water}{\left({}^2H/{}^1H\right)phytol} - 1 = \frac{\left(\delta^2H\right)water + 1}{\left(\delta^2H\right)phytol + 1} - 1 \quad (2)$$

As all epsilon and delta values are reported in per mil (‰) notation, this equation implies multiplication by 1000.

2.4. Bulk Isotope Compositions

Plant tissue for bulk $\delta^{15}N$ was subsampled from material collected for *n*-alkane extraction (Eley et al., 2014), which had been dried at 40 °C for 72 hr. Dried leaf material was cryogenically ground, and analyzed using a Delta XP ThermoFisher isotope-ratio mass spectrometer interfaced with a Costech elemental analyzer. For nitrogen isotopes, each batch of samples included replicate analyses of the in-house standard, casein ($\delta^{15}N$ = +6.15‰, previously calibrated against the International Atomic Energy Agency (IAEA) reference materials during an interlaboratory comparison exercise as part of EU Project SMT4-CT98-2236), which was used for drift correction. All $\delta^{15}N$ values are expressed relative to atmospheric nitrogen.

For δ^2H measurements of bulk leaf material, a series of in-house casein and collagen standards were analyzed to monitor for any instrument drift. The hydrogen reference gas was calibrated using IAEA 601 (benzoic acid), and an in-house benzoic acid standard previously calibrated against IAEA CH-7 (polyethylene) by the University of Reading. Samples for bulk δ^2H were measured in duplicate, and reported on the V-SMOW scale, with absolute differences between the measured replicates typically lower than 4‰ and not exceeding 7‰. We did not correct bulk hydrogen isotope values for exchangeable hydrogen contained in the cellulose and carbohydrate fractions of the leaf. As a result, it is likely that isotopic exchange occurred with ambient moisture in the laboratory air during sample preparation. However, all samples were prepared in the same laboratory at the same time. As a result, according to the principles of identical treatment, even though the absolute hydrogen isotope values will be affected by exchange with laboratory air, the relative differences between the plant species can still be compared.

2.5. Percentage Carbon and Nitrogen Content

The percentage of total C and N in the leaves of each species was quantified using a Carlo Erba EA 1108 Elemental Analyzer. During analysis, the combustion reactor was kept at a temperature of 900 °C. When a sample was dropped, a pulse of O_2 was injected to ensure that the sample underwent flash combustion. Helium was used as the carrier gas to transport the gas products of flash combustion through the combustion reactor. The resulting gases were separated on a chromatographic column and detected by a thermal conductivity detector (TCD). Acetanilide and sulphanilamide standards were analyzed at the start of each run and used to calibrate the instrument. These standards were also analyzed every ~10 samples, to monitor instrument performance. All data were blank corrected using empty tin capsules.

3. Results

3.1. Hydrogen Isotope Composition of Phytol

The δ^2H values of phytol vary by up to 63‰ among the seven sampled species (Figure 2; Table S1). In contrast to leaf wax *n*-alkane hydrogen isotope data (Eley et al., 2014), the most ^2H-depleted phytol value is observed for the evergreen dicot *A. portulacoides* (−361 ± 1‰), while the most ^2H-enriched is found in the C_4 monocot grass *S. anglica* (−298 ± 1‰). *Limonium vulgare*, a species which typically has one of the more ^2H-enriched *n*-C_{29} profiles (Eley et al., 2014), is among the more ^2H-depleted in terms of phytol (Figure 2). Statistical comparison of the δ^2H of phytol and leaf water (Table S1) reveals a positive relationship, although this is only significant at an 80% confidence interval (r = 0.5, P = 0.2, n = 7, Pearson's product moment correlation, Minitab v. 17). No relationship is observed between the δ^2H values of phytol and WA *n*-alkanes.

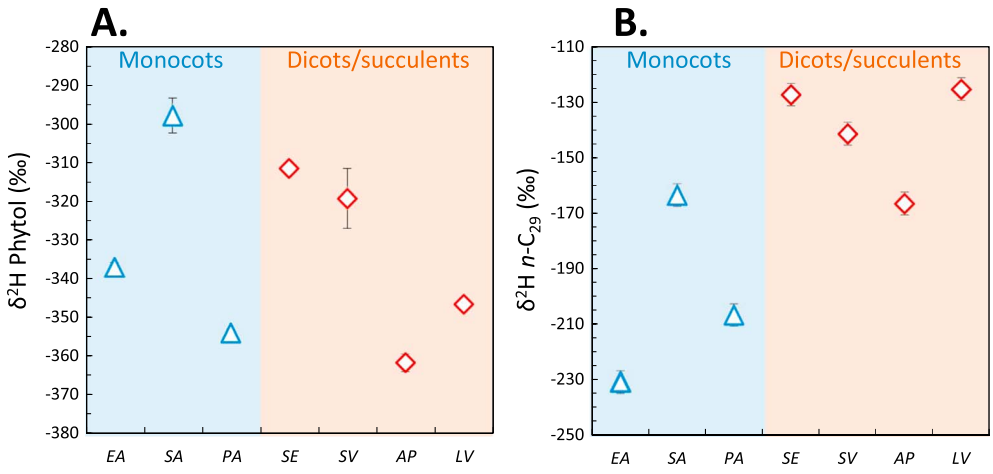

Figure 2. Interspecies variation in the δ^2H of (a) phytol and (b) *n*-C_{29} from samples collected in August 2012. *AP* = *Atriplex portulacoides*; *EA* = *Elytrigia atherica*; *LV* = *Limonium vulgare*; *PA* = *Phragmites australis*; *SE* = *Salicornia europaea*; *SA* = *Spartina anglica*; *SV* = *Suaeda vera*. Analytical error for repeat measurements of the same sample did not exceed 4‰.

3.2. Hydrogen Isotope Composition of Fatty Acids

δ^2H values of C_{16}, $C_{18:2}$ and $C_{18:3}$ are observed to vary by over 100‰ (Table S2; Figure 3). *E. atherica* has the most ^2H-depleted C_{16} value, while C_{16} from *S. vera* is the most ^2H-enriched. *L. vulgare* has the most ^2H-enriched linolenic acid value. Statistical comparison of $C_{16:0}$ and $C_{18:3}$ δ^2H with leaf water δ^2H reveals no relationship. However, $C_{18:2}$ has a positive relationship with leaf water δ^2H, although that relationship is only significant at a ~90% confidence interval (r = 0.7, P = 0.07 Pearson's product moment correlation). $C_{16:0}$ and $C_{18:3}$ $^2H/^1H$ values have a strong positive correlation (r = 0.8, P = <0.05, Pearson's product moment correlation), while $C_{18:2}$ is not correlated with either $C_{16:0}$ or $C_{18:3}$. Comparison of the FA δ^2H values to those of *n*-alkanes show that FA values are generally slightly ^2H-enriched compared to the *n*-alkanes and phytol, and depleted relative to leaf water. Overall, maximum interspecies variability in δ^2H values increases in the following order: leaf water < phytol < $C_{18:2}$ < $C_{18:3}$ < $C_{16:0}$ < *n*-alkanes.

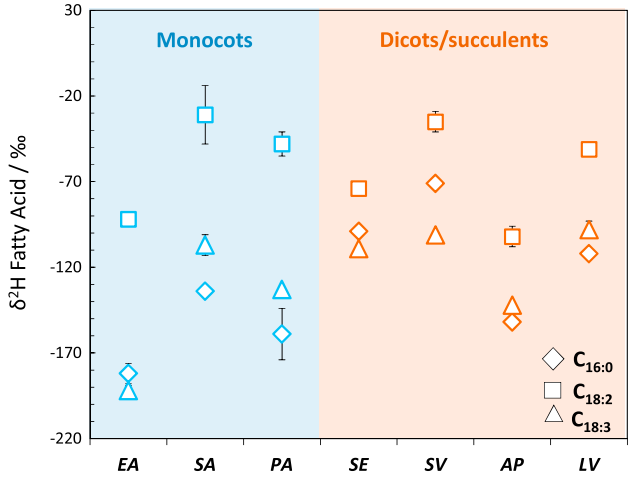

Figure 3. Comparison of the hydrogen isotope composition of palmitic, linoleic, and linolenic fatty acids. Abbreviations are as in Figure 2. Error bars show absolute differences between sample replicates.

3.3. Percentage Carbon and Nitrogen Content

The percentage carbon composition of bulk leaf tissue from the C_3 species at Stiffkey ranges from 21.6% (*S. europaea*, May 2012) to 45.5% (*P. australis*, September 2012). In a single sampling interval, %C varied among all the sampled plants by 10–23%. *P. australis* and *E. atherica* typically have the highest carbon content of all C_3 plants sampled in 2012 (Table S4). In contrast, the lowest %C content is consistently found in the annual succulent *S. europaea* (Table S4). %C in the leaves of the C_4 grass, *S. anglica*, during 2012 ranges from 35.9% to 41.1% (Table S4).

Nitrogen in the Stiffkey plants varies from ~0.5% to 4% depending upon the particular species and the sampling period. Among the grasses, *E. atherica* (C_3) consistently has the lowest nitrogen content, while *P. australis* (C_3) and *S. anglica* (C_4) generally range from 1% to 3%. Among the dicots and succulents, *L. vulgare* generally has a higher percentage of nitrogen than the stem succulent *S. europaea*. The amount of nitrogen varies with the dominant protective solutes produced, with plants preferentially producing nitrogenous compounds (dicots and succulents) having higher %N content than those preferentially producing carbohydrates (monocots; Figure 5).

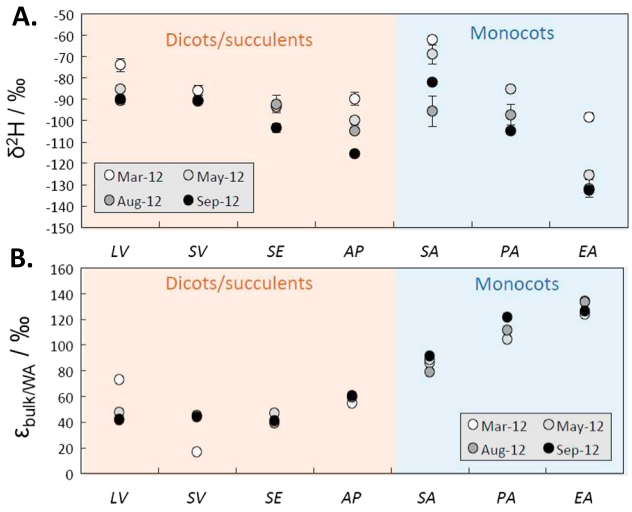

Figure 4. (a) Seasonal shifts in bulk hydrogen isotope composition and (b) difference between bulk and *n*-alkane hydrogen isotope composition for the 2012 growing season. Abbreviations are as in Figure 2.

3.4. Bulk Isotope Compositions

The bulk hydrogen isotope composition of all species sampled over the 2012 growing season ranges from −60‰ (*S. anglica*, March) to −133‰ (*E. atherica*, September; Table S4 and Figure 4). Interspecies variability in bulk $^{2}H/^{1}H$ ratio for each sampling interval exceeds 30‰, with the greatest range observed in May (56‰) and September (51‰). *L. vulgare* and *S. anglica* generally record the most ^{2}H-enriched bulk tissue, while *A. portulacoides* and *E. atherica* are typically the most ^{2}H-depleted. The greatest seasonal shifts in bulk tissue $\delta^{2}H$ are observed for the C_3 grass *E. atherica* and the C_4 grass *S. anglica*, which both show changes of 35‰. In contrast, the stem succulent *Salicornia europaea* has the most consistent bulk $\delta^{2}H$ values throughout the 2012 growing season, shifting by only 3‰. The nitrogen isotope composition of bulk leaf tissue varies between the C_3 and C_4 monocots and the dicots and succulents, with dicots and succulents generally having ^{15}N-enriched biomass relative to the monocots (Table S4 and Figure 4). Bulk leaf tissue from *A. portulacoides*, *S. vera*, and *S. europaea* are generally the most ^{15}N-enriched. In contrast, *E. atherica* and *L. vulgare* have the most ^{15}N-depleted leaf tissue. Among the monocots, the C_4 grass, *S. anglica*, has the most ^{15}N-enriched leaf tissue, and *E. atherica* has the most ^{15}N-depleted (Table S4).

4. Discussion

The hydrogen isotope composition of leaf wax lipids from individual plant species growing in a single geographic location can vary by over 100‰ throughout an entire growing season, despite limited variability in leaf water hydrogen isotope values (Eley et al., 2014; Oakes & Hren, 2016). This indicates that biochemical mechanisms may impart significant isotope effects on the $\delta^{2}H$ values of common plant biomarkers used in ecological and paleoclimatic investigations. Few studies have considered the potential

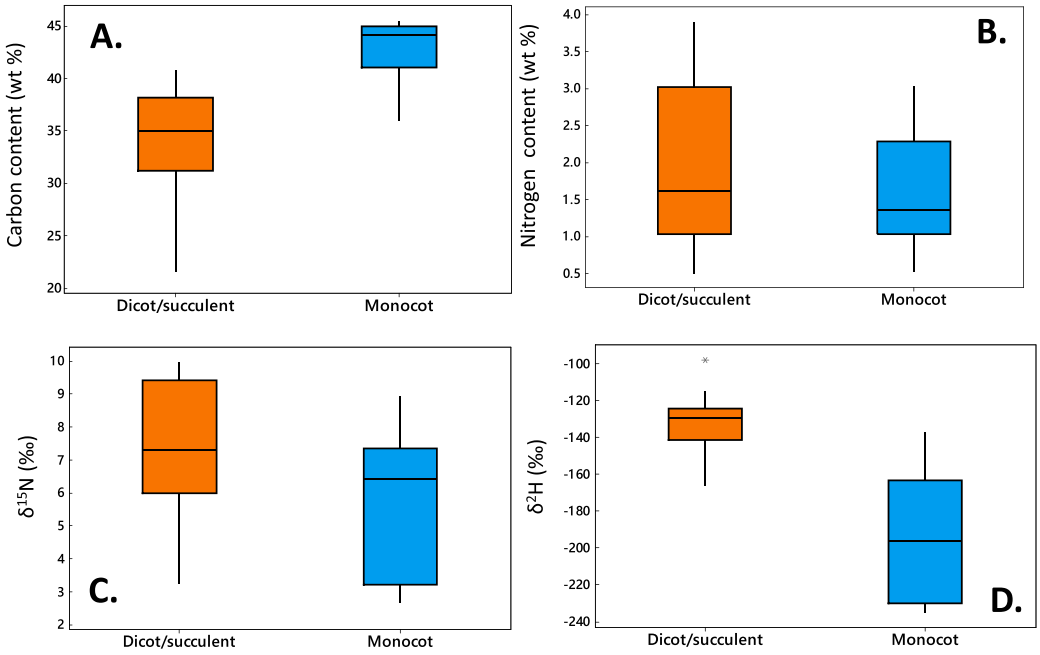

Figure 5. Differences in (a) percentage C content, (b) percentage N content, (c) nitrogen isotope ratios, and (d) the hydrogen isotope composition of *n*-C_{29}, between the monocots (blue) and the dicots and succulents (orange) analyzed as part of this study.

nature of these biochemical processes, or whether their actions differ among plant cell compartments. Here we consider a range of mechanisms that could influence the hydrogen isotope composition of both chloroplastic and cytosolic plant lipids, to provide a first-order identification of potential key areas for future investigations.

4.1. Hydrogen Isotope Composition of Phytol

Phytol is synthesized via the 1-deoxy-d-xylulose-5-phosphate (DOXP) pathway while hydrocarbons are synthesized via the acetogenic pathway (Chikaraishi et al., 2005, 2009; Chikaraishi & Naraoka, 2006; Sessions et al., 1999). Differences in isotope effects associated with biosynthetic reactions are expected between these two pathways (Chikaraishi et al., 2005, 2009; Sessions et al., 1999). Phytol from the C_4 grass *S. anglica* was found to be ^{2}H-enriched relative to the C_3 grass species. This confirms findings from previous studies of phytol hydrogen isotope composition of C_3, C_4 and CAM plants (Chikaraishi et al., 2004). However, although leaf water δ^2H from *S. anglica* was ^{2}H-enriched relative to the most ^{2}H-depleted leaf water from the C_3 monocot, *P. australis*, this variability was no larger than 29‰ between these species. Despite the overall positive relationship between phytol and leaf water δ^2H values, this variation in the hydrogen isotope composition of leaf water alone cannot account for the 62‰ difference in phytol δ^2H between these species. In C_3 plants, phytol is typically ^{2}H-depleted by ~300‰ to 330‰ in comparison to source water (Chikaraishi et al., 2009; Schmidt et al., 2003), although in our study the C_3 monocot, *P. australis*, the C_3 dicots, *L. vulgare*, and *S. vera*, all had $\varepsilon_{lw/phytol}$ values that were depleted by more than −350‰ (Figure 2). In C_3 plants, NADPH production generally proceeds by way of the action of ferroxidin-$NADP^+$ reductase (Fogel & Cifuentes, 1993). In contrast, some C_4 species also have the ability to generate NADPH from the activity of NADPH-linked malate enzymes, when malate is decarboxylated in the bundle sheath cells, while others produce aspartate as a first product of photosynthesis then decarboxylate with an NAD^+ malate-linked enzyme (Fogel & Cifuentes, 1993; Schmidt et al., 2003). Plants capable of generating NADPH from multiple sources tend to produce bulk tissue and cellulose that is ^{2}H-enriched relative to plants that can only utilize ferroxidin-$NADP^+$ (Fogel & Cifuentes, 1993). This enables C_4 plants to accumulate a larger pool of reduced coenzyme than C_3 species (Schmidt et al., 2003), reducing discrimination against ^{2}H in NADPH, and providing a plausible process to account for the ^{2}H-enriched phytol in the C_4 grass *S. anglica*. Additionally, photorespiration differs between C_3 and C_4 species, with the compartmentalization of CO_2 fixation in C_4 species resulting in ^{2}H-enrichment of H transferred by NADPH (Zhou et al., 2016). Again, this can account for the relative ^{2}H-enrichment of phytol in *S. anglica* relative to the C_3 species in this study.

Among the C_3 plants we studied, the fact that phytol δ^2H values have an identifiable positive relationship with the δ^2H of leaf water, and no relationship with *n*-alkane or bulk δ^2H, indicate that current photosynthate is an important H source for phytol synthesis (Sessions, 2006). However, interspecies variation in phytol δ^2H values among the C_3 plants (>40‰; Figure 2) is greater than that observed in leaf water, indicating that an additional mechanism operating in the chloroplast plays an important role in controlling these values. To date, studies have not identified biochemical differences in the MEP pathway among plant species (Phillips et al., 2008). We theorize that the mechanism or mechanisms driving our observed interspecies variation must take effect prior to the allocation of pyruvate to the MEP pathway, through different commitments of metabolites at branching points.

In contrast to the *n*-alkane hydrogen isotope data for these salt marsh plants (Eley et al., 2014), we observed a positive relationship ($r = 0.5$) between the δ^2H of leaf water and phytol, although this was only significant at an 80% confidence interval (potentially as a result of the small sample size, $n = 7$). The ^{2}H content of plant materials is a factor of both the hydrogen isotope composition of source water, and the site of their biosynthesis (Schmidt et al., 2003). The δ^2H of phytol, biosynthesized in the chloroplast, is likely to be a reflection of NADPH originating from photosynthetic water fission (Schmidt et al., 2003). Hydrogen species available for *n*-alkanes biosynthesis in the cytosol are likely to be sourced from a mixture of pools with distinct isotope compositions (for example, leaf water, carbohydrates, NADPH, and flavoproteins, Schmidt et al., 2003). As a result, the hydrogen isotope ratio of the hydride contained in NADPH in the cytosol is likely to have a different isotopic composition than in the chloroplast due to production in from the oxidative pentose phosphate pathway. We theorize that these differences result in the lack of a correlation between leaf water and *n*-alkane δ^2H as reported in Eley et al. (2014).

4.2. Hydrogen Isotope Composition of Fatty Acids

Variability in hydrogen isotope values for FAs from a single species at Stiffkey was typically between 50 and 100‰ (Figure 3), and higher among the monocots than the dicots and succulents. Similar levels of variability have been previously reported for microalgae (Chikaraishi et al., 2004). The distribution of ^{2}H along the FA carbon chain is variable, with different sources contributing H to specific sites on the molecule (Schwender et al., 2004). Quemerais et al. (1995) showed that hydrogen atoms on the methyl group of $C_{16:0}$ came from both the methyl group of pyruvate, and the hydride of NADPH. The methyl group of pyruvate, in turn, is linked to isotopomers 1, 6, and 6′ in glucose (Zhang et al., 1994). Quemerais et al. (1995) also found that the protons transferred by NADPH during the reduction of the malonyl-CoA carbonyl group were strongly related to cellular water, as a result of what has been described as "postmalonyl exchange." Critically, the deuterium distribution of the lipid component of plants appeared to be more strongly dominated by biochemical mechanisms than the isotopic composition of water absorbed and/or evaporated by plants (Quemerais et al., 1995). $C_{18:2}$ and $C_{18:3}$ FAs are the product of desaturation reactions of C_{18} in the endoplasmic reticulum (Billault et al., 2001; Chikaraishi et al., 2004). Studies have observed ^{2}H-depletion at the sites of desaturation (Billault et al., 2001), and increasing ^{2}H-enrichment in the residual oleate pool (Duan et al., 2002). It is plausible that because linolenic acid is a desaturation product of linoleic acid (Baillif et al., 2009; Chikaraishi et al., 2004) a similar explanation may account for the relative ^{2}H-enrichment of $C_{18:2}$ in comparison with $C_{18:3}$ from the Stiffkey plants (Figure 3).

What is more difficult to explain is the observed relationship between the δ^2H of leaf water and $C_{18:2}$. It is possible that the H atoms in $C_{18:2}$ are exchanging with cellular water (Baillif et al., 2009), and hence picking up a hydrogen signal from leaf water and/or transported photosynthate. It is unclear why this should affect $C_{18:2}$ more than $C_{18:3}$. The situation is further complicated by the existence of a significant relationship between $C_{16:0}$ and $C_{18:3}$, indicating that the H in their structures may be derived from a similar source. We hypothesize that as these plants are under stress (salinity, nutrient limitation, water availability), they may also produce $C_{18:3}$ from plant membranes (Dombrowski, 2003), to be converted into further protective compounds such as oxylipins (e.g., jasmonates, Wasternack, 2007). These membrane-derived $C_{18:3}$ FAs originate from chloroplast membranes (Wasternack, 2007) making it plausible that they contain H from a similar source to that incorporated into $C_{16:0}$ produced in the chloroplast (Figure 7).

While these factors may account for intramolecular variation in hydrogen isotope composition among the FAME homologues, the mechanisms responsible for the gross interspecies variation in FA δ^2H values require further exploration. For $C_{16:0}$ produced in the chloroplast we invoke similar mechanisms as for phytol above. For $C_{18:2}$ and $C_{18:3}$, the stereochemistry controlling the introduction of hydrogen atoms for all accessible stereogenic sites (and for each enantiontopic direction of stereogenic sites) is known to vary among organisms, resulting in shifts in the distribution of ^{2}H at the *pro-R* and *pro-S* sites (Baillif et al., 2009). As photosynthetic organisms have broadly similar biochemical mechanisms for the production of organic compounds (Billault et al., 2001; Chikaraishi et al., 2004; Sachse et al., 2012; Zhang & Sachs, 2007) it is possible that similar differences in stereochemistry may account for some of the species variability in FA δ^2H observed at Stiffkey. In addition, the potential for H exchange between acetate and cellular water is thought to be responsible for a previously observed strong transfer coefficient between the hydrogen attached to site 18 of FAs and H_2O (Baillif et al., 2009).

4.3. Hydrogen Isotope Composition of Bulk Plant Tissue: Implications for Membrane Metabolic Activity

The isotopic composition of bulk plant tissue is likely to be dominated by the carbohydrate signal, as ~75% of bulk plant tissue is made up from carbohydrates (Dungait et al., 2008). In this study, the maximum variation observed in bulk plant tissue hydrogen isotope composition (56‰) is only half of that recorded in *n*-alkanes (120‰, Eley et al., 2014). This indicates that while changes in the contribution of hydrogen from stored carbohydrate reserves may play a role in driving interspecies variation in *n*-alkane δ^2H, it is unlikely to be the only mechanism with a significant effect.

The maximum difference between bulk and *n*-alkane hydrogen isotope values is observed in the monocots (Figure 4). This may reflect the fact that monocots are utilizing discrete ^{2}H-depleted pools for acetogenic lipid synthesis. It is possible that this arises from variation between monocots and dicots in terms of metabolic

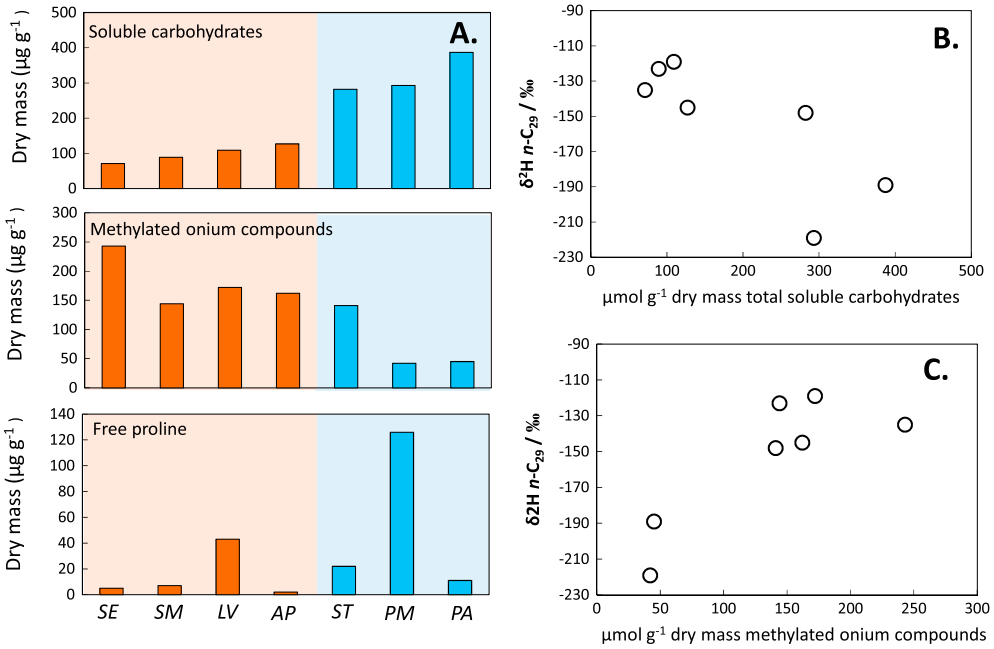

Figure 6. (a) Concentration of protective solutes produced by salt marsh species identical or comparable to those analyzed in this study (Briens & Larher, 1982): Abbreviations for SE, LV, AT, and PA are as in Figure 2; SM = *Suaeda maritima*; ST = *Spartina Townsendii*; PM = *Pucinellia maritima*. Relationship between the concentration of soluble carbohydrates (b) and methylated onium compounds (MOC) (c) and the hydrogen isotope composition of *n*-C_{29}.

activity across cell membranes. We theorize that plants with the greatest variability in metabolic activity across their cell membranes are more likely to create distinct pools with different levels of ^{2}H-enrichement (Brown et al., 2000). Drought and salinity stress, for example promote complex genetic modification of aquaporins (Skorupa-Kłaput et al., 2015). Equally, water stress can change the extent of protein phosphorylation, which also controls the number of aquaporins across different cellular compartments (Hasegawa et al., 2000; Maurel & Prado, 2017). Aquaglyceroporins (water channels that also transport solutes) can also be regulated by water stress (Hasegawa et al., 2000), which could further lead to the development of relatively ^{2}H-enriched or depleted cellular compartments. Applying this mechanism, those plants with relatively ^{2}H-enriched *n*-alkanes (i.e., in this case the dicots and succulents) would have a greater pool of ^{2}H in the cytosol. In contrast, those species with relatively ^{2}H-depleted *n*-alkanes (i.e., the monocots) must be sequestering ^{2}H in other cell compartments. The fact that we observe the greatest difference in bulk and *n*-alkane δ^2H in the monocots indicates that these plants may be sequestering deuterium in a cell compartment that is not available for acetogenic lipid synthesis but is observable when we analyze bulk leaf tissue.

4.4. Carbon and Nitrogen: Implications for the Role of Environmental Stress

Given that the preferential osmoregulatory solutes differ between monocots and dicots, we consider the role of synthesis and catabolism of solutes produced by the plants at Stiffkey a target for further study. If these biochemical adaptations to environmental stress from salinity, drought and/or root anoxia can influence the δ^2H of acetogenic lipids, they may also help account for the frequently observed ^{2}H-depletion of *n*-alkanes in monocots versus dicots (Liu et al., 2016; Sachse et al., 2012; Smith & Freeman, 2006). Such findings would have implications that extend far beyond salt marshes—these compounds are used by plants, bacteria, and even animals in response to many different stresses, such as drought, high light/UV intensity, and heavy metals (Slama et al., 2015; Szabados & Savouré, 2010; Yancey et al., 1982). The impact of osmoregulatory strategies may be influential when considering the hydrogen isotope composition of lipid biomarkers across a very broad range of other ecosystems. Earlier studies have observed that the monocot species sampled at Stiffkey preferentially accumulate carbohydrates, while the dicots and succulents are more likely to accumulate either nitrogenous compounds or a mix of nitrogenous and carbohydrate compounds (Briens

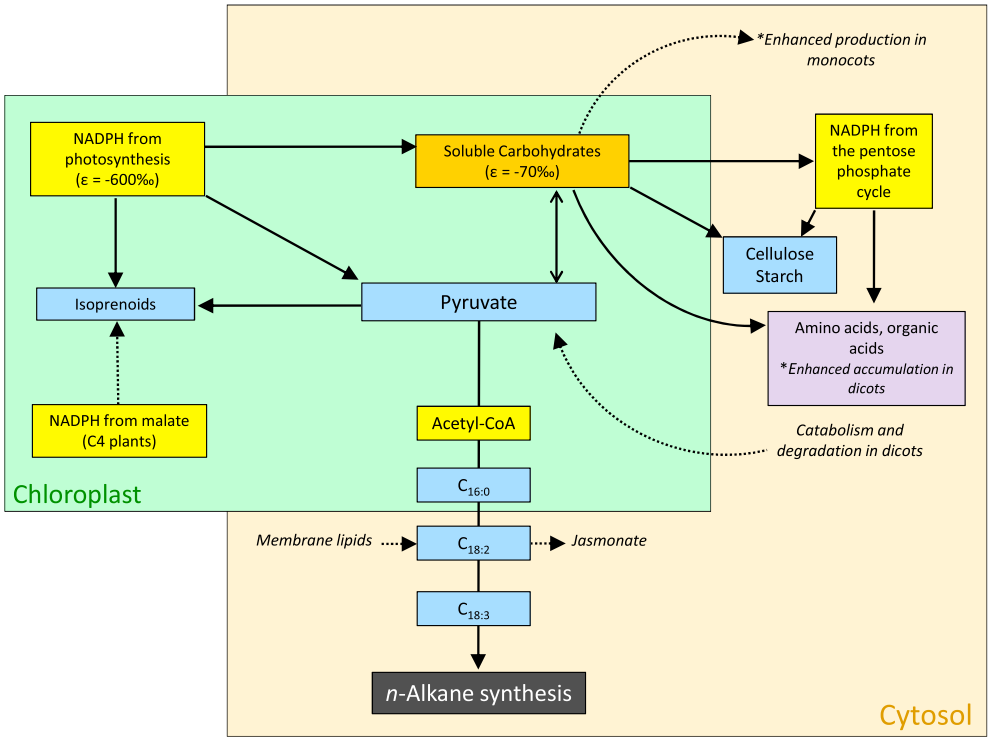

Figure 7. Simplified summary of the potential biochemical mechanisms that could influence isoprenoid and acetogenic lipid hydrogen isotope compositions. Assumed hydrogen isotope fractionation of NADPH (−600‰) is taken from Luo et al. (1991) and Zhang et al. (2009); the δ^2H of carbohydrates is from Ladd and Sachs (2012). The acetogenic pathway (FAs and alkanes) is abbreviated from Chikaraishi et al. (2004) and Shepherd and Griffiths (2006). Dashed arrows highlight the enhanced production of carbohydrates as compatible solutes in monocots and the potential for catabolism and degradation of proteins in dicots/succulents (Briens & Larher, 1982) to influence acetogenic lipid δ^2H. The potential membrane lipid source of $C_{18:2}$, linked to the production of jasmonate in stressed plants (Wasternack, 2007), is also shown.

& Larher, 1982; Figure 6). Percentage C and N observations from this study follow these trends, with monocots (accumulating carbohydrates) having overall higher concentrations of carbon, while dicots and succulents, which accumulate nitrogenous compounds, have higher percentages of nitrogen (Figure 5).

We find a clear negative relationship ($r = -0.8$, $p = 0.03$, Pearson moment correlation) between the concentration of soluble carbohydrates per gram of dry plant tissue and *n*-alkane δ^2H values, and a positive relationship ($r = 0.8$, $p = 0.02$, Pearson moment correlation) between *n*-alkane δ^2H and the concentration of nitrogenous methylated onium compounds (Figure 6). Previous research has considered whether the production of osmoregulatory solutes could have influenced the δ^2H of *n*-alkanes in mangroves through the allocation of pyruvate to the production of compounds such as asparagine, stachyose, glycine betaine, alanine, pinitol, and proline (Ladd & Sachs, 2012; Ladd & Sachs, 2015). If plants like our monocots have a high demand for carbohydrates to protect them from salinity (Slama et al., 2015), a greater proportion of hydrogen incorporated into pyruvate in these species will theoretically derive from NADPH. This would result in a ^2H-depletion in *n*-alkanes, as pyruvate is a precursor for acetogenic lipids (Ladd & Sachs, 2012; Ladd & Sachs, 2015; Figure 7). Likewise, as the dicot and succulent plant species at Stiffkey predominantly synthesize nitrogenous compounds, the ^2H-enrichment of their *n*-alkanes relative to the monocots could be influenced by the relatively higher input of carbohydrate-derived hydrogen to pyruvate as compared to the monocots (Figure 7). Variability in the relative proportion of carbohydrates to nitrogenous compounds among the dicots and succulents (Briens & Larher, 1982) could also potentially account for some of the interspecies differences in *n*-alkane δ^2H values among the dicot and succulent group.

Comparison of bulk nitrogen isotope composition and *n*-alkane weighted average δ^2H values revealed that there was a statistically significant strong positive relationship between foliar $\delta^{15}N$ and *n*-C_{29} δ^2H for the C_3 and C_4 monocots sampled ($r = 0.8$, $P < 0.05$, $n = 11$, Pearson moment correlation). In contrast, a negative

correlation was observed for the dicots and succulents ($r = -0.4$, $n = 14$, Pearson moment correlation), although this relationship was only significant at an ~85% confidence interval. While interpretation of the nitrogen isotope composition of plant materials is complicated by variation in terms of the source of form of N uptake, fractionation occurring during N absorption, any mycorrhizal symbioses, and during allocation within the plant (Evans, 2001; Werner & Schmidt, 2002), in this study we use bulk leaf nitrogen isotopes as an approximation of the relative abundance of nitrogenous compounds produced in plant leaves in response to environmental stress. Future studies should refine this approach through analysis of the compound-specific nitrogen isotope composition of amino acids and quantification of the concentration and relative abundance of the different protective osmolytes within the leaf.

The nitrogen isotope composition of proteins is more positive than other organic compounds found in phototrophic cells (Macko et al., 1986, 1987). Although we acknowledge the complexity of nitrogen isotope systematics in plants (e.g., Evans, 2001), for the purposes of this study, we regard the ^{15}N-enrichment of bulk leaf tissue in the dicots and succulents (relative to the monocots) as indicative of a greater abundance of osmoreguatory proteins and/or nitrogenous compounds in these plant functional types. Although the hydrogen isotope composition of proteins can vary considerably (e.g., in excess of 200‰ for amino acids (Fogel et al., 2016), in C3 plants they are typically ^{2}H-depleted relative to carbohydrates (Schmidt et al., 2003). Plants typically catabolize their protective proteins once environmental stresses decline (Araújo et al., 2011; Seki et al., 2007). Osmolytes have previously been viewed as stores of cellular reducing power available for use once the stress is reduced (Hasegawa et al., 2000). Catabolism and subsequent metabolism of proteins in stressed dicots and succulents may give rise to a relatively ^{2}H-depleted pool available for further respiration and secondary compound synthesis (Figure 7). In times of stress, an increase in the production of stress-related protein compounds could be accompanied by an enhanced consumption of ^{2}H-depleted pool of hydrogen for the synthesis of secondary compounds. This could lead to the negative relationship between foliar δ^{15}N and *n*-alkane δ^{2}H observed in this study.

The opposing relationship in the monocots could in part be simply due to their utilization of carbohydrates as preferred regulatory solutes. Alternatively, it could reflect the different sources of N used by Stiffkey salt marsh plants. Nitrogen available within the marsh includes nitrate (NO_3^-), ammonium (NH_4^+) and free amino acids (Henry & Jefferies, 2003; Quintã et al., 2015; Stewart & Lee, 1974). Different nitrogen sources impact upon proton activity in plants, with intracellular and cytoplasmic pH higher in species preferentially utilizing NO_3^- relative to those utilizing NH_4^+ (Raven, 2013). The use of different species of N also has an important influence on the NADPH budget of a plant cell. The uptake of NO_3^- requires NADPH to reduce it to NH_4^+, which can then be taken up by the GS-GOGAT pathway (Evans, 2001; Tcherkez & Hodges, 2008; Werner & Schmidt, 2002), while this is not required for direct uptake of $NH4^+$ and free amino acids. It is conceivable that some of the differences in acetogenic lipid hydrogen isotope composition observed between monocots and dicots might reflect NADPH budgets influenced by the uptake of different sources of N. Overall, these data indicate that the partitioning of deuterium across cell membranes (and ultimately in isoprenoid and acetogenic lipids) is strongly influenced by biological responses to environmental factors such as osmoregulation and N source. We recommend that future studies develop these theories further, quantifying the different osmoregulatory compounds in different plant species and evaluating their relationship with lipid hydrogen isotope values.

4.5. Paleoenvironmental Stress and Biomarker Isotope Records

Numerous studies have examined organic molecular carbon and hydrogen isotope records from stratigraphic sequences spanning major climate events such as the Younger Dryas (Rach et al., 2017) or the Paleocene-Eocene Thermal Maximum (PETM; e.g., Garel et al., 2013; Smith et al., 2007) to reconstruct linkages between atmospheric pCO_2, global temperature, and regional or global responses. Biomarker isotope records provide key insights into earth system responses to climatic perturbation, yet discrepancies between bulk organic, inorganic stable isotope and compound specific stable isotope data are common. If changes in atmospheric pCO_2, rapid cooling/warming, or factors such as fluctuations in leaf predation impart unique plant "stress", this may fundamentally change the allocation of precursor molecules to different organic pools within plant cells, with different metabolic pathways. Thus, these new results suggest that some of the discrepancies between compound-specific, bulk isotope and inorganic isotope records may derive from biologic responses to environmental stress and resource allocation. While complicating the interpretation

of paleoenvironmental organic molecular isotope records, these data also provide a glimpse of new possibilities to utilize paired geochemical records to tease apart a history of environmental change and biologic response through key climatic transitions in Earth's past.

5. Conclusions

This study provides a first-order evaluation of biochemical mechanisms that may influence higher plant interspecies biomarker δ^2H variation. Hydrogen isotope data from a range of compounds, including phytol and fatty acids, in comparison with the cytosol-derived *n*-alkanes indicate that mechanisms operating in the chloroplast can potentially drive interspecies δ^2H variation in both acetogenic and isoprenoid lipids. The C_4 monocot had the most ^2H-enriched phytol, potentially linked to the ability of C_4 plants to generate NADPH from the decarboxylation of malate or aspartate. We theorize that this additional hydrogen source could be an important factor driving observed variability in δ^2H among species with different carbon fixation pathways. The production of compatible solutes, for protection against environmental stress, appears to be linked to secondary compound δ^2H, with plants preferentially synthesizing carbohydrates (monocots) having ^2H-depleted *n*-alkanes relative to species that preferentially synthesize nitrogenous compounds (dicots and succulents). We assert that this ultimately reflects changes in the allocation of pyruvate, in response to the specific suite of protective compounds produced by a plant and may have a significant impact on the hydrogen isotope composition of acetogenic lipids. *n*-Alkane δ^2H values, measured in tandem with other parameters such as bulk $\delta^{15}N$ values and elemental (C, N) composition, may permit the identification of plant biochemical adaptation to environmental stress in modern settings with plants having higher N content or more positive $\delta^{15}N$ values likely to be producing nitrogenous compounds as compatible solutes under environmental stress. These insights provide new opportunities for investigating plant biochemistry in both modern species and the geologic record.

Competing Interests

The authors confirm that they have no conflicts of interest.

Data Availability Statement

All data generated or analyzed during this study are included in the supporting information associated with this article, or have been previously published in Eley et al. (2014). Should access to the previously published data be required, they will be made available following a reasonable request to the corresponding author.

Acknowledgments
The authors gratefully acknowledge the assistance of Annette Eley, Louise Jones, and Joseph Dillon during sample collection; B. Mayes and Jasmine Ross (James Hutton Institute) for technical and analytical support during data generation; and Y. Chikaraishi (Japan Agency for Marine-Earth Science and Technology), who provided valuable insights regarding the extraction of phytol. Yvette Eley was supported by the National Environmental Research Council [NE/P013112/1]. We also thank two anonymous referees for their comments; these greatly improved our manuscript.

References

Araújo, W. L., Tohge, T., Ishizaki, K., Leaver, C. J., & Fernie, A. R. (2011). Protein degradation—An alternative respiratory substrate for stressed plants. *Trends in Plant Science*, *16*, 489–498.

Ashraf, M., & Foolad, M. R. (2007). Roles of glycine betaine and proline in improving plant abiotic stress resistance. *Environmental and Experimental Botany*, *59*(2), 206–216. https://doi.org/10.1016/j.envexpbot.2005.12.006

Baillif, V., Robins, R. J., Le Feunteun, S., Lesot, P., & Billault, I. (2009). Investigation of fatty acid elongation and desaturation steps in Fusarium lateritium by quantitative two-dimensional deuterium NMR spectroscopy in chiral oriented media. *The Journal of Biological Chemistry*, *284*(16), 10,783–10,792. https://doi.org/10.1074/jbc.M807826200

Billault, I., Guiet, S., Mabon, F., & Robins, R. (2001). Natural deuterium distribution in long-chain fatty acids is nonstatistical: A site-specific study by quantitative ^2H NMR spectroscopy. *Chembiochem: A European Journal of Chemical Biology*, *2*(6), 425–431. https://doi.org/10.1002/1439-7633(20010601)2:6<425::AID-CBIC425>3.0.CO;2-Z

Briens, M., & Larher, F. (1982). Osmoregulation in halophytic higher plants: A comparative study of soluble carbohydrates, polyols, betaines and free proline. *Plant, Cell & Environment*, *5*, 287–292.

Brown, L. S., Needleman, R., & Lany, J. K. (2000). Origins of deuterium kinetic isotope effects on the proton transfers of the bacteriorhodopsin photocycle. *Biochemistry*, *39*(5), 938–945. https://doi.org/10.1021/bi9921900

Chikaraishi, Y., Matsumoto, K., Ogawa, N. O., Suga, H., Kitazato, H., & Ohkouch, N. (2005). Hydrogen, carbon and nitrogen isotopic fractionations during chlorophyll biosynthesis in C3 higher plants. *Phytochemistry*, *66*(8), 911–920. https://doi.org/10.1016/j.phytochem.2005.03.004

Chikaraishi, Y., & Naraoka, H. (2006). Carbon and hydrogen isotope variation of plant biomarkers in a plant–soil system. *Chemical Geology*, *231*(3), 190–202. https://doi.org/10.1016/j.chemgeo.2006.01.026

Chikaraishi, Y., Naraoka, H., & Poulson, S. R. (2004). Hydrogen and carbon isotopic fractionations of lipid biosynthesis among terrestrial (C3, C4 and CAM) and aquatic plants. *Phytochemistry*, *65*(10), 1369–1381. https://doi.org/10.1016/j.phytochem.2004.03.036

Chikaraishi, Y., Tanaka, R., Tanaka, A., & Ohkouch, N. (2009). Fractionation of hydrogen isotopes during phytol biosynthesis. *Organic Geochemistry*, *40*(5), 569–573. https://doi.org/10.1016/j.orggeochem.2009.02.007

Cormier, M. A., Werner, R. A., Sauer, P. E., & Gröcke, D. R. (2018). ^2H-fractionations during the biosynthesis of carbohydrates and lipids imprint a metabolic signal on the δ^2H values of plant organic compounds. *New Phytologist*, *218*(2), 479–491. https://doi.org/10.1111/nph.15016

Diefendorf, A. F., Freeman, K. H., Wing, S. L., & Graham, H. V. (2011). Production of *n*-alkyl lipids in living plants and implications for the geologic past. *Geochimica et Cosmochimica Acta*, *75*(23), 7472–7485. https://doi.org/10.1016/j.gca.2011.09.028

Dombrowski, J. E. (2003). Salt stress activation of wound-related genes in tomato plants. *Plant Physiology*, *132*(4), 2098–2107. https://doi.org/10.1104/pp.102.019927

Douglas, P. M. J., Pagani, M., Brenner, M., Hodell, D. A., & Curtis, J. H. (2012). Aridity and vegetation composition are important determinants of leaf-wax δD values in southeastern Mexico and Central America. *Geochimica et Cosmochimica Acta*, *97*, 24–45. https://doi.org/10.1016/j.gca.2012.09.005

Duan, J.-R., Billault, I., Mabon, F., & Robins, R. (2002). Natural deuterium distribution in fatty acids isolated from peanut seed oil: A site-specific study by quantitative ^{2}H NMR spectroscopy. *Chembiochem: A European Journal of Chemical Biology*, *3*(8), 752–759. https://doi.org/10.1002/1439-7633(20020802)3:8<752::AID-CBIC752>3.0.CO;2-G

Dungait, J. A. J., Docherty, G., Straker, V., & Evershed, R. P. (2008). Interspecific variation in bulk tissue, fatty acid and monosaccharide δ^{13}C values of leaves from a mesotrophic grassland plant community. *Phytochemistry*, *69*(10), 2041–2051. https://doi.org/10.1016/j.phytochem.2008.03.009

Eley, Y., Dawson, L., Black, S., Andrew, J., & Pedentchouk, N. (2014). Understanding 2H/1H systematics of leaf wax n-alkanes in coastal plants at Stiffkey saltmarsh, Norfolk, UK. *Geochimica et Cosmochimica Acta*, *128*, 13–28. https://doi.org/10.1016/j.gca.2013.11.045

Evans, R. D. (2001). Physiological mechanisms influencing plant nitrogen isotope composition. *Trends in Plant Science*, *6*(3), 121–126. https://doi.org/10.1016/S1360-1385(01)01889-1

Feakins, S. J., Kirby, M. E., Cheetham, M. I., Ibarra, Y., & Zimmerman, S. R. H. (2014). Fluctuation in leaf wax D/H ratio from a southern California lake records significant variability in isotopes in precipitation during the late Holocene. *Organic Geochemistry*, *66*, 48–59. https://doi.org/10.1016/j.orggeochem.2013.10.015

Fischer, C. R., Bowen, B. P., Pan, C., Northen, T. R., & Banfield, J. F. (2013). Stable-isotope probing reveals that hydrogen isotope fractionation in proteins and lipids in a microbial community are different and species-specific. *ACS Chemical Biology*, *8*(8), 1755–1763. https://doi.org/10.1021/cb400210q

Fogel, M. L., & Cifuentes, L. A. (1993). Isotope fractionation during primary production. In M. H. Engel & S. A. Macko (Eds.), *Organic geochemistry* (pp. 73–98). US: Springer.

Fogel, M. L., Griffin, P. L., & Newsome, S. D. (2016). Hydrogen isotopes in individual amino acids reflect differentiated pools of hydrogen from food and water in Escherichia coli. *Proceedings of the National Academy of Sciences of the United States of America*, *113*(32), E4,648–E4,653. https://doi.org/10.1073/pnas.1525703113

Gao, L., Edwards, E. J., Zeng, Y., & Huang, Y. (2014). Major evolutionary trends in hydrogen isotope fractionation of vascular plant leaf waxes. *PLoS One*, *9*(11), e112610. https://doi.org/10.1371/journal.pone.0112610

Garcés, R., & Mancha, M. (1993). One-step lipid extraction and fatty acid methyl esters preparation from fresh plant tissues. *Analytical Biochemistry*, *211*(1), 139–143. https://doi.org/10.1006/abio.1993.1244

Garcin, Y., Schwab, V. F., Gleixner, G., Kahmen, A., Todou, G., Séné, O., et al. (2012). Hydrogen isotope ratios of lacustrine sedimentary n-alkanes as proxies of tropical African hydrology: Insights from a calibration transect across Cameroon. *Geochimica et Cosmochimica Acta*, *79*, 106–126. https://doi.org/10.1016/j.gca.2011.11.039

Garel, S., Schnyder, J., Jacob, J., Dupuis, C., Boussafir, M., Le Milbeau, C., et al. (2013). Paleohydrological and paleoenvironmental changes recorded in terrestrial sediments of the Paleocene–Eocene boundary (Normandy, France). *Palaeogeography, Palaeoclimatology, Palaeoecology*, *376*, 184–199. https://doi.org/10.1016/j.palaeo.2013.02.035

Good, A. G., & Zaplachinski, S. T. (1994). The effects of drought stress on free amino acid accumulation and protein synthesis in *Brassica napus*. *Physiologia Plantarum*, *90*(1), 9–14. https://doi.org/10.1111/j.1399-3054.1994.tb02185.x

Harwood, J. L. (1988). Fatty acid metabolism. *Annual Review of Plant Physiology and Plant Molecular Biology*, *39*(1), 101–138. https://doi.org/10.1146/annurev.pp.39.060188.000533

Hasegawa, P. M., Bressan, R. A., Zhu, J.-K., & Bohnert, H. J. (2000). Plant cellular and molecular responses to high salinity. *Annual Review of Plant Physiology and Plant Molecular Biology*, *51*(1), 463–499. https://doi.org/10.1146/annurev.arplant.51.1.463

Hayes, J. M. (2001). Fractionation of carbon and hydrogen isotopes in biosynthetic processes. *Reviews in Mineralogy and Geochemistry*, *43*, 255–277.

Henry, H. A. L., & Jefferies, R. L. (2003). Plant amino acid uptake, soluble N turnover and microbial N capture in soils of a grazed Arctic salt marsh. *The Journal of Ecology*, *91*(4), 627–636. https://doi.org/10.1046/j.1365-2745.2003.00791.x

Hobbie, E., & Werne, R. A. (2004). Intramolecular, compound-specific, and bulk carbon isotope patterns in C3 and C4 plants: A review and synthesis. *The New Phytologist*, *161*(2), 371–385. https://doi.org/10.1111/j.1469-8137.2004.00970.x

Hren, M. T., Pagani, M., Erwin, D. M., & Brandon, M. (2010). Biomarker reconstruction of the early Eocene paleotopography and paleoclimate of the northern Sierra Nevada. *Geology*, *38*(1), 7–10. https://doi.org/10.1130/G30215.1

Kahmen, A., Schefuß, E., & Sachse, D. (2013). Leaf water deuterium enrichment shapes leaf wax n-alkane δD values of angiosperm plants I: Experimental evidence and mechanistic insights. *Geochimica et Cosmochimica Acta*, *111*, 39–49. https://doi.org/10.1016/j.gca.2012.09.003

Kar, N., Garzione, C. N., Jaramillo, C., Shanahan, T., Carlotto, V., Pullen, A., et al. (2016). Rapid regional surface uplift of the northern Altiplano plateau revealed by multiproxy paleoclimate reconstruction. *Earth and Planetary Science Letters*, *447*, 33–47. https://doi.org/10.1016/j.epsl.2016.04.025

Kunst, L., & Samuels, L. (2009). Plant cuticles shine: advances in wax biosynthesis and export. *Current Opinion in Plant Biology*, *12*, 721–727. https://doi.org/10.1016/j.pbi.2009.09.009

Ladd, N., & Sachs, J. P. (2012). Inverse relationship between salinity and n-alkane δD values in the mangrove Avicennia marina. *Organic Geochemistry*, *48*, 25–36. https://doi.org/10.1016/j.orggeochem.2012.04.009

Ladd, S. N., & Sachs, J. P. (2015). Hydrogen isotope response to changing salinity and rainfall in Australian mangroves. *Plant, Cell & Environment*, *38*(12), 2674–2687. https://doi.org/10.1111/pce.12579

Liu, J., Liu, W., An, Z., & Yang, H. (2016). Different hydrogen isotope fractionations during lipid formation in higher plants: Implications for paleohydrology reconstruction at a global scale. *Scientific Reports*, *6*(1), 19711. https://doi.org/10.1038/srep19711

Luo, Y.-H., Steinberg, L., Suda, S., Kumazawa, S., & Mitsui, A. (1991). Extremely low D/H ratios of photoproduced hydrogen by cyanobacteria. *Plant & Cell Physiology*, *32*, 897–900.

Macko, S. A., Estep, M. L. F., Engel, M. H., & Hare, P. E. (1986). Kinetic Fractionation of Stable Nitrogen Isotopes During Amino-Acid Transamination. *Geochimica Et Cosmochimica Acta*, *50*(10), 2143–2146. https://doi.org/10.1016/0016-7037(86)90068-2

Macko, S. A., Fogel, M. L., Hare, P., & Hoering, T. C. (1987). Isotopic fractionation of nitrogen and carbon in the synthesis of amino acids by microorganisms. *Chemical Geology: Isotope Geoscience Section*, *65*(1), 79–92. https://doi.org/10.1016/0168-9622(87)90064-9

Maurel, C., & Prado, K. (2017). Aquaporins and leaf water relations. In F. Chaumont & S. D. Tyerman (Eds.), *Plant aquaporins* (pp. 155–165). Cham, Switzerland: Springer International Publishing. https://doi.org/10.1007/978-3-319-49395-4_7

McInerney, F. A., Helliker, B. R., & Freeman, K. H. (2011). Hydrogen isotope ratios of leaf wax n-alkanes in grasses are insensitive to transpiration. *Geochimica et Cosmochimica Acta*, *75*(2), 541–554. https://doi.org/10.1016/j.gca.2010.10.022

Newberry, S. L., Kahmen, A., Dennis, P., & Grant, A. (2015). *n*-Alkane biosynthetic hydrogen isotope fractionation is not constant throughout the growing season in the riparian tree *Salix viminalis*. *Geochimica et Cosmochimica Acta*, *165*, 75–85. https://doi.org/10.1016/j.gca.2015.05.001

Niedermeyer, E. M., Forrest, M., Beckmann, B., Sessions, A. L., Mulch, A., & Schefuß, E. (2016). The stable hydrogen isotopic composition of sedimentary plant waxes as quantitative proxy for rainfall in the West African Sahel. *Geochimica et Cosmochimica Acta*, *184*, 55–70. https://doi.org/10.1016/j.gca.2016.03.034

Oakes, A. M., & Hren, M. T. (2016). Temporal variations in the δD of leaf n-alkanes from four riparian plant species. *Organic Geochemistry*, *97*, 122–130. https://doi.org/10.1016/j.orggeochem.2016.03.010

Pagani, M., Pedentchouk, N., Huber, M., Sluijs, A., Schouten, S., Brinkhuis, H., et al. (2006). Arctic hydrology during global warming at the Palaeocene/Eocene thermal maximum. *Nature*, *442*(7103), 671–675. https://doi.org/10.1038/nature05043

Parida, A. K., & Das, A. B. (2005). Salt tolerance and salinity effects on plants: A review. *Ecotoxicology and Environmental Safety*, *60*(3), 324–349. https://doi.org/10.1016/j.ecoenv.2004.06.010

Phillips, M. A., León, P., Boronat, A., & Rodríguez-Concepción, M. (2008). The plastidial MEP pathway: Unified nomenclature and resources. *Trends in Plant Science*, *13*(12), 619–623. https://doi.org/10.1016/j.tplants.2008.09.003

Quemerais, B., Mabon, F., Naulet, N., & Martin, G. J. (1995). Site-specific isotope fractionation of hydrogen in the biosynthesis of plant fatty acids. *Plant, Cell & Environment*, *18*(9), 989–998. https://doi.org/10.1111/j.1365-3040.1995.tb00609.x

Quintã, R., Hill, P. W., Jones, D. L., & Santos, R. (2015). Uptake of an amino acid (alanine) and its peptide (trialanine) by the saltmarsh halophytes Salicornia europaea and Aster tripolium and its potential role in ecosystem N cycling and marine aquaculture wastewater treatment. *Ecological Engineering*, *75*, 145–154. https://doi.org/10.1016/j.ecoleng.2014.11.049

Rach, O., Kahmen, A., Brauer, A., & Sachse, D. (2017). A dual-biomarker approach for quantification of changes in relative humidity from sedimentary lipid D/H ratios. *Climate of the Past; Katlenburg-Lindau*, *13*(7), 741–757. https://doi.org/10.5194/cp-13-741-2017

Raven, J. A. (2013). Half a century of pursuing the pervasive proton. In U. Lüttge, W. Beyschlag, D. Francis, & J. Cushman (Eds.), *Progress in Botany* (pp. 3–34). Berlin, Heidelberg: Springer.

Rhodes, D., Handa, S., & Bressan, R. A. (1986). Metabolic changes associated with adaptation of plant cells to water stress. *Plant Physiology*, *82*(4), 890–903. https://doi.org/10.1104/pp.82.4.890

Sachse, D., Billault, I., Bowen, G. J., Chikaraishi, Y., Dawson, T. E., Feakins, S. J., et al. (2012). Molecular paleohydrology: Interpreting the hydrogen-isotopic composition of lipid biomarkers from photosynthesizing organisms. *Annual Review of Earth and Planetary Sciences*, *40*(1), 221–249. https://doi.org/10.1146/annurev-earth-042711-105535

Sachse, D., Gleixner, G., Wilkes, H., & Kahmen, A. (2010). Leaf wax n-alkane δD values of field-grown barley reflect leaf water δD values at the time of leaf formation. *Geochimica et Cosmochimica Acta*, *74*(23), 6741–6750. https://doi.org/10.1016/j.gca.2010.08.033

Schefuss, E., Kuhlmann, H., Mollenhauer, G., Prange, M., & Pätzold, J. (2011). Forcing of wet phases in southeast Africa over the past 17,000 years. *Nature*, *480*(7378), 509–512. https://doi.org/10.1038/nature10685

Schmidt, H.-L., Werner, R. A., & Eisenreich, W. (2003). Systematics of ^{2}H patterns in natural compounds and its importance for the elucidation of biosynthetic pathways. *Phytochemistry Reviews*, *2*(1-2), 61–85. https://doi.org/10.1023/B:PHYT.0000004185.92648.ae

Schwender, J., Ohlrogge, J., & Shachar-Hill, Y. (2004). Understanding flux in plant metabolic networks. *Current Opinion in Plant Biology*, *7*(3), 309–317. https://doi.org/10.1016/j.pbi.2004.03.016

Seki, M., Umezawa, T., Urano, K., & Shinozaki, K. (2007). Regulatory metabolic networks in drought stress responses. *Current Opinion in Plant Biology*, *10*(3), 296–302. https://doi.org/10.1016/j.pbi.2007.04.014

Sessions, A. L. (2006). Seasonal changes in D/H fractionation accompanying lipid biosynthesis in Spartina alterniflora. *Geochimica et Cosmochimica Acta*, *70*(9), 2153–2162. https://doi.org/10.1016/j.gca.2006.02.003

Sessions, A. L., Burgoyne, T. W., Schimmelmann, A., & Hayes, J. M. (1999). Fractionation of hydrogen isotopes in lipid biosynthesis. *Organic Geochemistry*, *30*(9), 1193–1200. https://doi.org/10.1016/S0146-6380(99)00094-7

Shepherd, T., & Griffiths, D. W. (2006). The effects of stress on plant cuticular waxes. *New Phytologist*, *171*, 469–499. https://doi.org/10.1111/j.1469-8137.2006.01826.x

Skorupa-Kłaput, M., Szczepane, J., Kurnik, K., Tretyn, A., & Tyburski, J. (2015). The expression patterns of plasma membrane aquaporins in leaves of sugar beet and its halophyte relative, Beta vulgaris ssp. maritima, in response to salt stress. *Biologia*, *70*, 467–477.

Slama, I., Abdelly, C., Bouchereau, A., Flowers, T., & Savouré, A. (2015). Diversity, distribution and roles of osmoprotective compounds accumulated in halophytes under abiotic stress. *Annals of Botany*, *115*(3), 433–447. https://doi.org/10.1093/aob/mcu239

Smith, F. A., & Freeman, K. H. (2006). Influence of physiology and climate on δD of leaf wax n-alkanes from C 3 and C 4 grasses. *Geochimica et Cosmochimica Acta*, *70*(5), 1172–1187. https://doi.org/10.1016/j.gca.2005.11.006

Smith, F. A., Wing, S. L., & Freeman, K. H. (2007). Magnitude of the carbon isotope excursion at the Paleocene–Eocene thermal maximum: The role of plant community change. *Earth and Planetary Science Letters*, *262*(1–2), 50–65. https://doi.org/10.1016/j.epsl.2007.07.021

Stewart, G. R., & Lee, J. A. (1974). The role of proline accumulation in halophytes. *Planta*, *120*(3), 279–289. https://doi.org/10.1007/BF00390296

Szabados, L., & Savouré, A. (2010). Proline: A multifunctional amino acid. *Trends in Plant Science*, *15*(2), 89–97. https://doi.org/10.1016/j.tplants.2009.11.009

Tcherkez, G., & Hodges, M. (2008). How stable isotopes may help to elucidate primary nitrogen metabolism and its interaction with (photo) respiration in C3 leaves. *Journal of Experimental Botany*, *59*(7), 1685–1693. https://doi.org/10.1093/jxb/erm115

Tierney, J. E., & deMenocal, P. B. (2013). Abrupt shifts in Horn of Africa hydroclimate since the Last Glacial Maximum. *Science*, *342*(6160), 843–846. https://doi.org/10.1126/science.1240411

Tierney, J. E., Lewis, S. C., Cook, B. I., LeGrande, A. N., & Schmidt, G. A. (2011). Model, proxy and isotopic perspectives on the East African Humid Period. *Earth and Planetary Science Letters*, *307*(1-2), 103–112. https://doi.org/10.1016/j.epsl.2011.04.038

von Wettstein-Knowles, P., Olsen, J. G., & McGuire, K. A. (2006). Fatty acid synthesis. *The FEBS Journal*, *273*, 695–710.

Wasternack, C. (2007). Jasmonates: An update on biosynthesis, signal transduction and action in plant stress response, growth and development. *Annals of Botany*, *100*(4), 681–697. https://doi.org/10.1093/aob/mcm079

Werner, R. A., & Schmidt, H.-L. (2002). The in vivo nitrogen isotope discrimination among organic plant compounds. *Phytochemistry*, *61*(5), 465–484. https://doi.org/10.1016/S0031-9422(02)00204-2

Wing, B. A., & Halevy, I. (2014). Intracellular metabolite levels shape sulfur isotope fractionation during microbial sulfate respiration. *Proceedings of the National Academy of Sciences of the United States of America*, *111*(51), 18,116–18,125. https://doi.org/10.1073/pnas.1407502111

Yancey, P. H., Clark, M. E., Hand, S. C., Bowlus, R. D., & Somero, G. N. (1982). Living with water stress: Evolution of osmolyte systems. *Science*, *217*(4566), 1214–1222. https://doi.org/10.1126/science.7112124

Zhang, B.-L., Quemerais, B., Martin, M. L., Martin, G. J., & Williams, J. M. (1994). Determination of the natural deuterium distribution in glucose from plants having different photosynthetic pathways. *Phytochemical Analysis: PCA*, *5*(3), 105–110. https://doi.org/10.1002/pca.2800050304

Zhang, X., Gillespie, A. L., & Sessions, A. L. (2009). Large D/H variations in bacterial lipids reflect central metabolic pathways. *Proceedings of the National Academy of Sciences of the United States of America*, *106*(31), 12,580–12,586. https://doi.org/10.1073/pnas.0903030106

Zhang, Z., & Sachs, J. P. (2007). Hydrogen isotope fractionation in freshwater algae: I. Variations among lipids and species. *Organic Geochemistry*, *38*(4), 582–608. https://doi.org/10.1016/j.orggeochem.2006.12.004

Zhou, Y., Grice, K., Stuart-Williams, H., Hocart, C., Gessler, A., & Farquhar, G. (2016). Hydrogen isotopic differences between C3 and C4 land plant lipids: Consequences of compartmentation in C4 photosynthetic chemistry and C3 photorespiration. *Plant, Cell & Environment*, *39*(12), 2676–2690. https://doi.org/10.1111/pce.12821